CELLULOSE HYDROGELS WITH OXIDIZED TANNIC ACID PARTICLES – SYNTHESIS AND CHARACTERIZATION

A Thesis

Presented to the Faculty of the Graduate School

of Cornell University

In Partial Fulfillment of the Requirements for the Degree of

Master of Science

by

Shiyao Hong

August 2021

ABSTRACT

This thesis reports on the synthesis of a hydrogel made from oxidized tannic acid (OTA) nanoparticles and TEMPO-oxidized cellulose nanofibers ((TOCN). We prepared the OTA nanoparticles by oxidizing tannic acid (TA) under slightly alkaline conditions. Fourier-transform infrared spectroscopy (FTIR) and Thermogravimetric Analysis (TGA) were used to probe the chemical and structural changes of the OTA nanoparticles during the oxidation. The morphology of OTA particles was observed using a Scanning Electron Microscopy (SEM). OTA nanoparticles were added into a TOCN suspension to form TOCN/OTA hydrogels at 60 ℃ for 28 hours. In addition to hydrogels, TOCN/OTA aerogels were also prepared through freeze-drying. We noted that the hydroxyl groups on the surface of TOCN and OTA could form intra- and interchain hydrogen bonds, while the flexible cellulose nanofibers could form high physical entanglements. TGA spectra verified the improved thermal stability of the cellulose aerogel when OTA nanoparticles were incorporated. We also investigated the effect of weight ratio of TOCN/OTA on the thermal and viscoelastic properties of the hydrogels and aerogels. Samples prepared at higher TOCN/OTA weight ratios exhibited higher thermal stability. Rheological tests indicate that TOCN/OTA hydrogels act as elastic solids under cyclical deformation. An optimal weight ratio of TOCN/OTA was determined. TOCN/OTA hydrogels were prepared from natural resources, and through ‘green’ methods, and it is expected that these new materials could find applications in medical and hygienic products as well as in environmental remediation processes.

BIOGRAPHICAL SKETCH

Caroline Hong was born and raised in Zhejiang Province, China. She graduated from Hongda High School in June of 2015. The following fall, she entered the Department of Textile at Donghua University, where she received her Bachelor of Science in Textile Engineering. In her senior year, she got the opportunity to study abroad in Fiber Science in the Department of Human Ecology at Cornell University, which was sponsored by China Scholarship Council.

In August of 2019, Caroline Hong began her Master of Science program in Fiber Science at Cornell University. She joined Professor Juan Hinestroza's research group. With the help of her advisor and minor committee member, she conducted her research and completed her master thesis in August of 2021. After completing her MS degree, Caroline will continue her Ph. D in the Department of Forest Biomaterials at North Carolina State University.

ACKNOWLEDGMENTS

First and foremost, I am extremely grateful to my advisor, Professor Juan Hinestroza. His professional and precise attitude toward research was influential in shaping my experiment methods and critiquing my results. His kind guidance and continuous encouragement have helped me overcome different challenges in work and daily life.

I would also like to thank my minor committee member, Professor Andrej Singer, from Material Science, for his invaluable advice, continuous support, and patience during my MS study.

I would like to thank all the members of the department of Fiber Science. Their kind help and support have made my study and life at Cornell a wonderful time.

Finally, I would like to express my gratitude to my family and friends. Without their tremendous understanding and encouragement in the past few years, it would be impossible for me to complete my study.

TABLE OF CONTENTS

LIST OF FIGURES

1. INTRODUCTION

A hydrogel is a three-dimensional, water-swollen, crosslinked network of polymer chains. The swell ability of hydrogels in water derives from their hydrophilic groups, while the water insolubility derives from their crosslinks. Hydrogels can be classified into chemically and physically crosslinked hydrogels. Chemically crosslinked hydrogels have permanent bonds, namely covalent bonds. Physically crosslinked hydrogels have temporary and reversible connections, such as hydrogen bonds, van der Waals interactions, and physical entanglements. Hydrogels are generally formed from the polymerization of hydrophilic monomers or the modification of existing polymers. Over the past two decades, researchers have developed various fabrication techniques for the hydrogels, enhanced their inherent properties, and introduced novel functions to the hydrogels. Hydrogels find use in different fields, including hygienic, agricultural, and pharmaceutical products.[1] Synthetic hydrogels are generally more durable and stronger than natural hydrogels. However, as the consumption of fossil fuels dramatically increased, the design and synthesis of multifunctional natural hydrogels became a promising project to remedy environmental challenges, detect ecological changes, treat pollution, and engineer biomedical innovations.[2] This thesis describes the synthesis and characterization of a cellulose-based physically crosslinked hydrogel that incorporates oxidized tannic acid (OTA) particles.

Cellulose based hydrogels are promising materials with diverse applications, such as biomedical, pharmaceutical, and adhesives, due to their biocompatible, antibacterial, and antioxidant properties. Cellulose and tannins are synthesized from renewable and vast natural resources.

Cellulose, a term initially coined by Payen (1838) to refer to purified cellulosic materials, is the most abundant biomass on earth, followed by hemicellulose, lignin, and tannins.[3] It is found in various sources, including plants (cellulose contributes approximately 33% of all plant materials), several animals, fungi, bacteria (such as Acetobacter, Acanthamoeba), unicellular plankton, algae (such as Valonia, Chaetamorpha), and minerals.[4] Payen initially isolated cellulose from wood and determined its chemical constitution[5]. Advancing research discovered its structure, reactivity, and derivatives, resulting in large-scale fabrication and broader application. A turning point to realize the industrial production of cellulose was in 1870; Hyatt Manufacturing Company produced the

first thermoplastic polymer, celluloid, based on the reaction of cellulose with nitric acid to form cellulose nitrate.[5] Later on, the production of regenerated cellulose, particularly rayon (1890s) and cellophane (1912), followed. After that, Hermann Staudinger pioneered vital research to determine the polymeric structure of cellulose in 1920.[6] Recently, the production methods and property control techniques have allowed for a broader application of cellulose.

Tannins are precipitate proteins found in many trees and plants, such as black wattle or black mimosa bark (Acacia mearnsii), quebracho wood (Schinopsis balansae or lorentzii), oak bark (Quercus spp.), chestnut wood pieces (Castanea sativa), algarrobilla chileno, tara, and the bark of several species of pines and firs. Tannins are manufactured by a chloroplast-derived organelle: the tannosome. They are mainly located in the vacuoles or surface wax of plants; thus, they can protect against light and predation without affecting the plant metabolism. People have used tannins as leathering tanning for millennia, but the actual tannin extraction industry started in the 1850s to meet the need for black dyes. The leather industry underwent rapid expansion by taking advantage of tannin extract in leather production in the early 1900s. The use of vegetable tannins in the leather industry reached its zenith in 1946 due to the demand of leather materials for shoes during the two world wars. In the years following, tannin sales for leather steadily dwindled due to a reduction in demand following the development of synthetic counterparts for shoes and a shift in market choice for shoes. However, in the 1960s and 1970s, people discovered many new applications of tannins, from varnish primers for metals to cement superplasticizers. Furthermore, scientists found a use for tannins in wood adhesives. They are now quickly becoming an environmentally friendly alternative to some synthetic compounds that have challenges meeting formaldehyde emission regulations. Moreover, the biocompatible, antiviral, antioxidant, and therapeutic virtues of tannins promote their application in other varying fields, such as pharmaceuticals, medicine, animal feed, and beverages.[7]

2. PROJECT BACKGROUND

2.1.Nanocellulose

Nanocellulose is a collective name used to describe nanoscale fibrils of extended cellulose chains: cellulose nanofibers (CNFs), and their crystalline parts: cellulose nanocrystals (CNCs). The crystalline cellulose has a tensile strength up to 10 GPa, which is greater than that of cast iron, and a stiffness up to 220 GPa, which is comparable to that of Kevlar.[8,9]

CNCs are also known as cellulose nanowhiskers or nanorods depending upon their cross-section. CNCs are highly crystalline (typically 54-88% in crystallinity), short (typically <500 nm), and thin (normally 3-20 nm wide), with a low aspect ratio.[9,10] CNCs are usually obtained through acid hydrolysis, and other acid-free methods such as oxidation reaction, enzymatic hydrolysis and sub/supercritical water or ionic liquid assisted techniques. Among them, widely used sulfuric acid hydrolysis and oxidative methods are the major focus for scale-up efforts.

CNFs are flexible and entangled (typically 0.1-3 μm long, 4-60 nm wide), with a high aspect ratio, high surface area, and extensive hydroxyl groups.[9,6,11] CNFs are typically extracted from lignocellulosic materials found in wood pulp. Top-down methods for CNFs isolation commonly involve enzymatic, chemical, and/or physical methodologies that rip larger fibers into nanofibers. These processes may dramatically change the original surface chemistry and interface interactions and consume large amounts of energy. Enzymatic or chemical pretreatments are more cost-effective and efficient ways to extract cellulose nanofibers. Take carboxymethylation and TEMPO (2,2,6,6-tetramethylpiperidine-1-oxyl)-mediated oxidation as examples. They could introduce charged carboxylate groups to the cellulose fibrils, promoting the swelling of the fibers by electrostatic repulsion. The well-swelled fibers help loosen the interfibrillar hydrogen bonds and facilitate the nanofibrillation during the subsequent mechanical treatments. The nanofibers obtained through this method are called TEMPO-oxidized CNFs, abbreviated as TOCNs.[12]

The nanoscale fibrils exhibit high surface areas, and strong chemical and physical interactions with various species. The abundant hydroxyl groups present on the cellulose chains make it an ideal material for chemical modification. Therefore, research work on incorporating nanocellulose into

sustainable, biocompatible, and multifunctional materials while maintaining its mechanical properties has recently received attention.[6]

2.1.1. Chemical structure

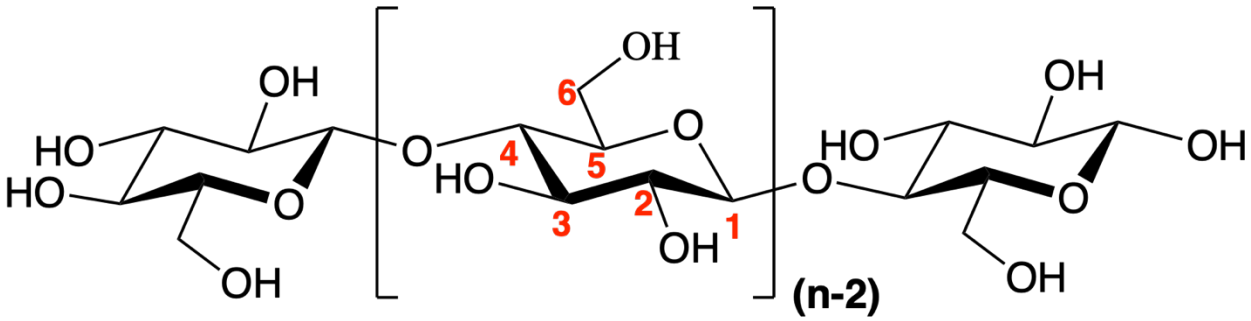

Figure 2.1: Basic chemical structure of cellulose; n = 2000 to 27000, depending on the cellulose source material.[13]

Cellulose is a linear chain composed of thousands of β (1-4) linked D-glucose units ($C_6H_{10}O_5$). As Figure 2.1 shows, two glucose rings are linked through an oxygen covalently bonded to C-1 of one glucose unit and C-4 of the adjoining unit. The glucose units are referred as anhydroglucose units (AGU) when a molecular of water is lost. The reactivity of cellulose is ascribed mainly to the three hydroxyl (OH) groups, one primary group at C-6 and two secondary groups at C-2 and C-3 in each of the AGU unit. The reactivity of three hydroxyl groups ranks as: OH group located at C-6 > OH group located at C-2 > OH group located at C-3. A large amount of intra- and interchain hydrogen bonds provide cellulose materials with good strength, stability, as well as insolubility in water and most organic solvents.[4,9] Cellulose swells as it absorbs water in its amorphous regions while not dissolving in water. Therefore, it provides an ideal template for tailoring hydrogels.

2.1.2. TEMPO-mediated oxidation

Ample surface hydroxy groups in CNFs allow for a wide variety of modification techniques such as adsorption, esterification, acetylation, acylation, cationization, silylation, carbonation, TEMPO-mediated oxidation, grafting, click chemistry, and fluorescent labeling.[14] Dufresne et al. reviewed these modifications in detail. Here, we focus on the recent development of TEMPO-mediated oxidation and the non-covalent adsorption of TOCNs.

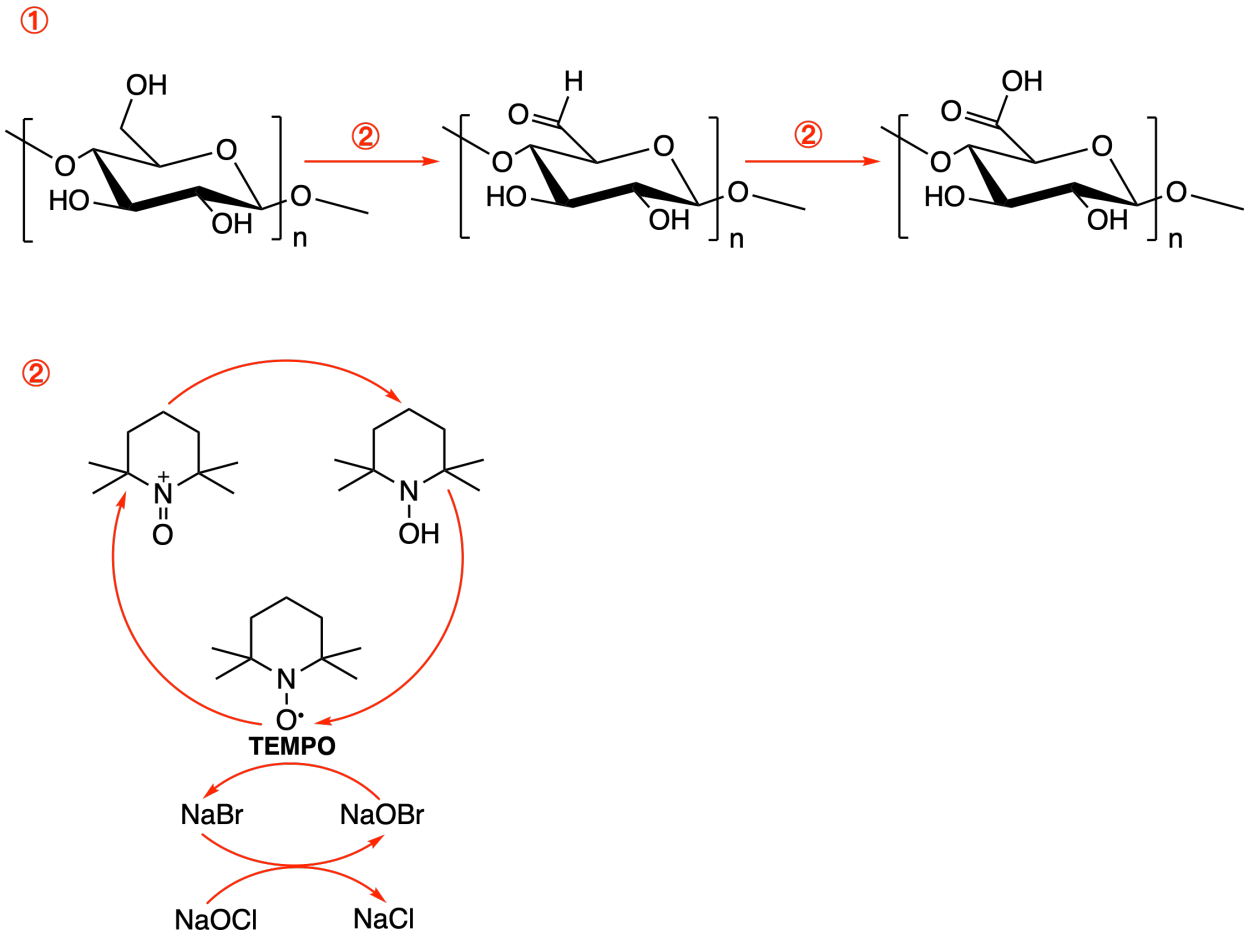

Figure 2.2: TEMPO-mediated oxidation of primary hydroxyls to carboxyl groups.

TEMPO-mediated oxidation of cellulose was initially reported by De Nooy et al. TEMPO could regioselectively oxidize the hydroxymethyl groups of polysaccharides, while the remaining secondary hydroxyls reamin unaffected.[15] TEMPO is water-soluble, commercially available, and stable nitroxyl radical. As Figure 2.2 shows, the oxidation of cellulose takes place in the TEMPO/sodium bromide (NaBr)/sodium hypochlorite (NaClO) system in water at pH 10-11:

1. NaClO oxidizes NaBr to sodium hypobromite (NaOBr).
2. It converts TEMPO into a nitrosonium ion which regioselectively oxidizes the hydroxymethyl groups on cellulose to aldehyde by reducing itself into hydroxylamine.[16]
3. Carboxylation occurs because hydroxylamine can regenerate the nitrosonium ion, which completes the catalytic cycle.[17] The position-selective oxidation occurs at the

hydroxymethyl groups due to the steric hindrance of the four methyl groups attached per TEMPO molecule.[2]

The resultant bio-based material contains great amounts of carboxylate groups that are densely, regularly, and regioselectively present on the surface of the TOCN. Through mechanical disintegration, individual TOCN with a width of 3-4 nm and a length of 0.5-2 μm can be stably dispersed in water due to electrostatic repulsion between the anionically charged groups.[16]

TOCNs obtained from this process are in the form of a sodium salt (-COO-Na+), and this salt can be converted into free carboxyl groups (-COOH) by HCl. TOC-COOH exhibits low dispersibility in water due to the formation of inter- and intrachain hydrogen bonds. At the same time, it is more dispersible in polar aprotic organic solvents such as N, N-dimethylacetamide (DMAc), N, N-dimethylformamide (DMF), 1,3-dimethyl-2-imidazolidinone (DMI), and 1-methyl-2-pyrrolidinone (NMP). Contrarily, TOC-COONa shows low dispersibility in these solvents and only formed a stable dispersion, at the individual nanofibril level, in dimethylsulfoxide (DMSO).[18]

The rheological properties for TOCN suspensions or TOCN hydrogels are important in fabrication and application; hence it is interesting to discuss both forms of bulk TOCNs and their composites. Geng et al. investigated the rheological characterization of TOCN hydrogels as functions of concentration and ionic strength. The suspensions behaved like Newtonian fluids below a lower concentration level (0.1%). In contrast, the suspensions exhibited an evident shear thinning behavior at higher concentrations due to the increased disentanglements of long fibers.[19] Liao et al. reported the flow curves of the TOCNs, showing that a Newtonian plateau was followed by shear thinning. They proposed a rheological model combining a power law and cross model to describe the viscoelastic behavior of TOCNs at different shear rates. [20]

2.1.3. Non-covalent adsorption

The surface of nanocellulose can be tailored by ionic electrostatic interaction, hydrogen bonds, and van der Waals forces.

Significant amounts of sodium C6-carboxylate groups are present regularly and regioselectively on the surface of TOCN. These groups can be converted to protonated carboxyl groups (TOC-COOH) by acids, other metals and alkylammonium carboxylate groups through ionic exchange in water. In addition to hydrogen ion exchange, many metal ions such as Al^{3+}, Ca^{2+}, Cu^{2+}, Co^{2+}, Na^{+}, Ag^{+}, can be adsorbed onto TOCN. The resultant metal-decorated TOCN composites exhibit enhanced mechanical properties and provide superior deodorant performances.[21,22] Masruchin et al. reported that the higher valences of cations incorporated in the TOCN hydrogels improved their mechanical properties.[21] Apart from metals, TOCN nanocomposites based on oxides are also of great interest. As TOCNs support the precipitation of TiO_2, the resultant nanocomposite TOCN/TiO_2 can be used as an adsorbent for brilliant blue (BB) dye and it has a higher adsorption capacity in a slightly alkaline medium system.[23]

Hydrogen bonds also foster the formation of TOCN-based nanocomposites. Poly (acrylamide) (PAM)/TOCN nanocomposites in the forms of films and hydrogels show excellent mechanical properties when compared to PVA/TOCNs or starch/TOCNs. As Kurihara et al. proposed, attractive interactions might form at the interfaces between TOCN and PAM, and an anionic charge might contribute to mechanical reinforcement.[24] Similarly, Masruchin reported that poly (N-isopropylacrylamide) (PNIPAAm)/TOCN hydrogels with dual responsiveness to temperature and pH were promising materials for drug delivery.[25] Such strategies are promising because they allowed the preservation of the inherent anionic charges on nanocelluloses while interacting with other polymers. The added polymer chains enhanced the formation of network, therefore, the viscosity and storage modulus were markedly improved and easily tuned by varying the chain length.[12]

Multicomponent systems of TOCN and metal ions interacting via ionic electrostatic interactions and hydrogen bonds have been reported. Yamada et al. studied the growth of dispersed hydroxyapatite (HAp) crystals highly intertwined with TOCNs in the presence of Ca^{2+}. The ionic coordination bonds between Ca^{2+} and the carboxyl groups on the surface of TOCN led to an interaction with HAp. Comparing to other substrates such as agar and bacterial cellulose (BC) gel, the resultant TOCN-based hybrid composite provided a higher surface area and better durability.[26] Alginate modified nanocellulose hydrogels in the presence of Ca^{2+} promote the mineralization,

and hence have great potential in bone tissue engineering. The presence of an entangled nanofiber network ensures dimensional stability, good mechanical properties, and the hydrophilic characteristics of the resultant gels. Compared to CNCs/alginate, TEMPO-oxidized cellulose nanocrystals, and (TOCNCs)/alginate hydrogels, TOCN/alginate gels showed the best compatibility conditions for bio-adhesion and growth of fibroblasts cells.[27] Abouzeid et al. reported on the biomimetic mineralization of 3-D printed TOCN/alginate scaffolds for bone tissue. Ca^{2+} improved the crosslinking from partially crosslinked TOCN/alginate hydrogel to fully crosslinked hydrogel improving their printability. In addition, the resultant material showed high thixotropic behavior and compressive strength.[28] Furthermore, Niu et al. reported that the introduction of Fe^{3+} into PAM/TOCN hydrogels could improve their self-recovery, shape memory, and tensile strength. The hydrogen bonds between PAM and TOCNs significantly improved the mechanical strength, toughness, and fatigue resistance of the hydrogels.[29,30]

Freeze-thawing is also a common way to assemble hybrid TOCN composites. Repeated freezing and thawing could form the microporous and physically crosslinked TOCN/PVA hydrogels. The cycles of freeze-thaw are essential to increase the crystallinity and hence, the hydrogel mechanical properties.[31] Curcumin can also be incorporated into PVA/TOCN hydrogels to promote wound healing.[32]

2.2.Tannic acid

Tannins are the fourth most abundant source of aromatic biomolecules; they are found aplenty in the bark as well as wood and, in smaller amounts, in the leaves and fruits of various plants and trees.[33,34] Tannins are polyphenolic, and hence a good alternative for the elaborating chemicals and as building blocks for polymeric materials. Tannins in plants play essential roles in defending against biological threats and protecting from UV rays, free radicals, and dryness.[3,35]

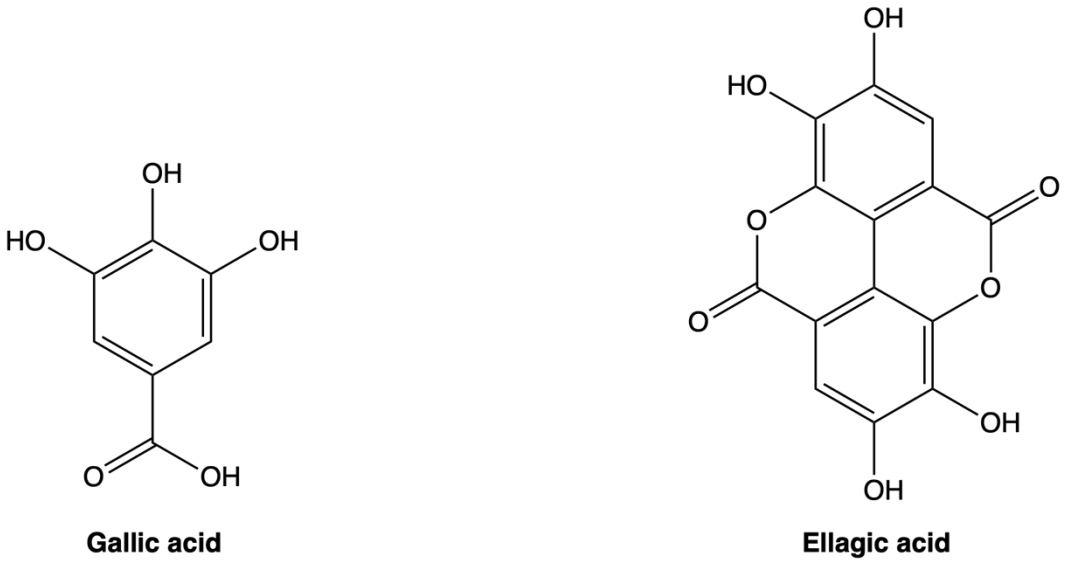

Figure 2.3: Chemical structure of gallic acid and ellagic acid.

Tannins fall under three categories: hydrolysable, condensed, and complex tannins. Hydrolysable tannins consist of a carbohydrate at the molecule's center, esterified with phenolic groups such as gallic acid and ellagic acid (Figure 2.3). As the name indicates, they can be hydrolyzed by weak acids/bases to generate carbohydrates and phenolic acids. Tannic acid (TA) (Figure 2.4) is the most common hydrolysable tannin. Hydrolysable tannins are mainly used in the leather tanning industry and have antimicrobial applications.[35] However, they exhibit a low level of phenol substitution, nucleophilicity, and their macromolecular structure can be changed by the extraction techniques. Hydrolysable tannins make up to less than 10% of the worldwide commercial tannin production and have a higher price.[35] Another genus of tannins is condensed tannins, making up more than 90% of the worldwide commercial tannin production due to their higher chemical reactivity.[3,35]

Condensed tannins (also known as proanthocyanidins, polyflavonoid tannins), including procyanidins, prodelphinidins, profisetinidins, and prorobinetidins, are formed from polyhydroxy-flavan-3-ols or flavan-3,4-diols (leucoanthocyanidin).[35,36] They are not susceptible to be cleaved by hydrolysis, although most of them are water-soluble. The last one is complex tannins, which consist of both ellagitannin units and flavonoid units. However, they are limited in applications due to their complex structure and relatively low abundance.[3]

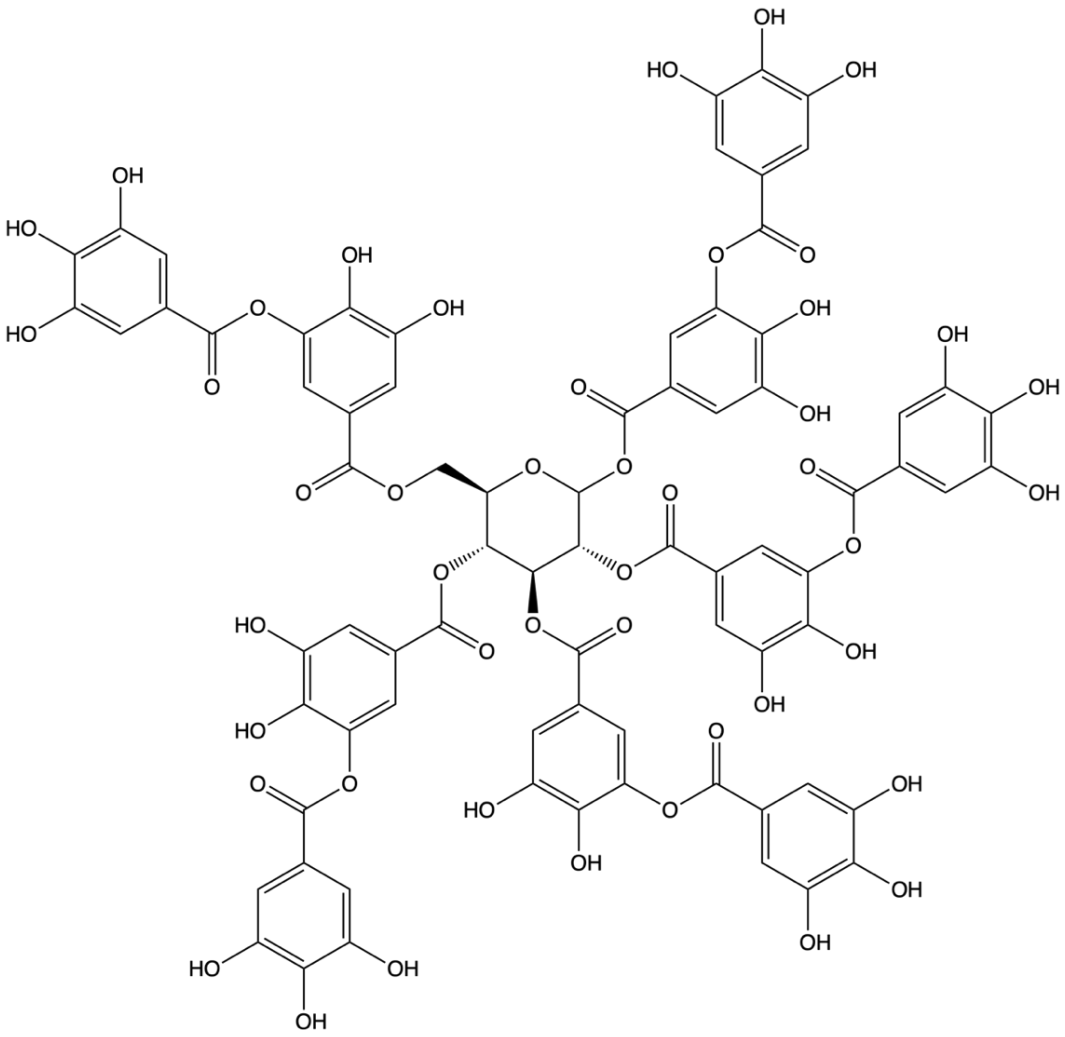

Figure 2.4: Chemical structure of tannic acid.

The yields of conventional extraction methods for tannins are low (6-39%) depending on the plants' species and the types of solvents used.[35] Recently, other novel extraction methods, such as using microwaves, ultrasonics, or sub/supercritical water-assisted techniques, are used.[35]

2.2.1. Oxidized Tannic Acid

Tannic acid has a central glucose molecule derivatized at its hydroxyl groups with one or more galloyl residues. The hydroxyl groups on TA can be easily oxidized into carbonyl groups. The oxidized tannic acid (OTA) exhibits different morphologies and sizes depending on the synthesis process. Kamarainen et al. probed the effect of the base species, pH, and agitation time on OTA formation. They induced agitation and oxidation by orbital shaking, rendering enough contact with oxygen.[37] Then, the OTA particles were ready to precipitate because of the lower water-solubility of carbonyl groups than the hydroxyl groups.

Similar to TA, OTA can react with metals via ionic coordination. Additionally, OTA-based composites have been reported, using gelatin and chitosan as templates. First, gelatin or chitosan crosslinked with OTA via a Schiff base reaction between the amino groups ($-NH_2$) and carbonyl groups (=O) on OTA. Double crosslinks could be selectively induced by adding Fe^{3+} to form metal coordination. The functional composites possess enhanced tenacity, strength, and rapid self-healing ability.[38,39] Although various morphologies and new functional groups have been introduced for OTA, their chemical and physical properties have not been extensively discussed.

2.2.2. Tannic Acid-based Composites

Tannic acid has a polyphenolic structure, with abundant hydroxyl groups and π systems. TA acts as a reducing agent, hydrogen donor, and as a quencher of singlet oxygen at its natural acidic pH due to the redox behavior of phenol groups.[40] These properties give rise to their antioxidant, antimutagenic, anticarcinogenic properties and harbors inhibitory action against skin, lungs, and forestomach tumors caused by polycyclic aromatic hydrocarbon carcinogens and N-methyl-N-nitrosourea in mice.[41,40,42,43] TA also imparts UV protection due to its π-system. Moreover, adsorption of metals can be achieved by catechol types metal complexation; hence TA can be used

as a crosslinker and adhesive. TA can be versatilely modified due to its hydroxyl groups, forming hydrogen bonds with organic compounds, achieving metal chelation with metals or metal oxides, and attaining various chemical modifications such as acylation, esterification, and substitution by ammonia.

Chemical and/or physical interactions between tannic acid and metals to create composites have been widely reported. Using TA as a reducing and stabilizing agent, Liu et al. reported developing an enhanced anti-bacterial TA-Ag nanoparticles (NPs) film by reducing Ag^{+} to metal Ag NPs using the hydroxyl groups on TA.[44] TA can also be modified with metals via catechol-like coordination. Fan et al. reported multifunctional supramolecular hydrogels where TA was linked to polymers, including polyvinylpyrrolidone (PVP), poly(ethylene glycol) (PEG), poly(sodium 4-styrenesulfonate) (PSS), and poly(dimethyldiallylammonium chloride) (PDDA), and Fe^{3+} through hydrogen bonds and ionic coordination.[45] In addition to anti-bacterial behavior, metal-based TA composites exhibit good electrochemical properties. A conductive hydrogel with good mechanical properties was synthesized by Hao et al. In a TA-Ag dual catalytic system, PAM was formed from acrylamide (AM) through radical polymerization initiated by TA-Ag. Meanwhile, TA formed crosslinks with cellulose via hydrogen bonds. The resultant composite showed good stretchability, self-adhesion, anti-bacterial properties, and self-recovery.[46]

Tannin-organic hybrid-like materials can be formed by intimately mixing, covalently or physically crosslinking. For example, to prepare PVA and TA composites, TA can act as a strong crosslinker, and promote the coagulation and gelation of PVA via hydrogen bonding at elevated temperatures.[47] Reinforced mechanical properties of PVA/TA hydrogels can be further achieved through freeze-thawing while preserving its innate anti-bacterial and antioxidant performance.[48] In addition to physical interactions, PVA/TA composite films can be prepared through the esterification of hydroxyl groups.[49] The phenolic structure of TA brings great potential to interact with various polymers to form multifunctional composites and broaden its application in different fields.

Hu et al. mixed CNCs with TA through oxidation and oligomerization. They added decylamine (DA) which reacted with TA through a Schiff base formation/Michael-type addition. They

improved the hydrophobicity of cellulose nanocrystals, and the contact angle increased from 21 to 74 ° with the addition of plant polyphenols.[50] Shao et al. reported a mussel-inspired cellulose nanocomposite hydrogel based on the coordinate bonds among TA@CNCs, Poly (acrylic acid) (PAA), and metal ions Al^{3+}. The resultant hydrogel possesses self-healing, adhesiveness, and strain-sensitive properties.[51] Later on, Shao et al. further improved TA@CNCs and PVA nanocomposite hydrogels. The intricately interconnected networks induced high toughness, self-healing dynamic adhesion, and strain-stiffening properties.[52] Inspired by the pioneering work of Hu et al., a similar modification was reported by Shrestha et al. for the modification of TOCN, where headecylamine (HAD) replaced DA and epoxy added as a crosslinker. In addition to hydrophobicity, properties including dispersion, adhesion, mechanical strength, and thermal stability were enhanced in comparison to unmodified TOCN-epoxy.[53]

3. MATERIALS AND METHODS

3.1.Materials

TEMPO-oxidized cellulose nanofibers (aqueous suspension) were purchased from the University of Maine. Tannic acid ($C_{76}H_{52}O_{46}$, 1701.20 g/mol) was purchased from Sigma Aldrich (Saint Louis, MO, USA), and sodium hydroxide (NaOH) pellets were purchased from Macron Fine Chemicals (Sweden).

3.2.Methods

3.2.1. Preparation of OTA

First, 2 wt.% tannic acid solution was prepared by dissolving tannic acid particles into DI water in glass beakers. The pH of the solution was adjusted to 7.8 by adding 1 M NaOH. Then the beakers were covered with perforated plastic wrap to ensure continuous oxygenation of the solution. The oxidized tannic acid particles precipitated under shaking (200 rpm, RT) after ca. 8 h. At last, OTA particles were collected through centrifugation and freeze-dried for ca. 24 h.

3.2.2. Preparation of hydrogels and aerogels

TOCN/OTA hydrogels were prepared by adding OTA particles into a 5 wt.% TOCN aqueous suspension. Initially, 20 ml of a sonicated TOCN suspension was put into a beaker and mixed with OTA particles. The weight ratios of TOCN (dry weight): OTA used in the hydrogel formation were 1:1, 1:2, 1:3. The mixture was then sonicated and magnetically stirred for ca. 1 h to ensure homogeneity. Finally, the mixture was transferred into a petri-dish (100x10 mm) to mold a suitable shape for rheological tests. The hydrogel was formed under 60°C for 28 h. The corresponding aerogel was prepared by freeze-drying. The hydrogel was put in a freezer at -20°C for ca. 12 h and then was lyophilized in a Labconco freeze dryer (Millrock Technology Inc. Kingston, New York, USA) under vacuum ($<133x10^{-3}$ MBar) at -60°C for 24 h.

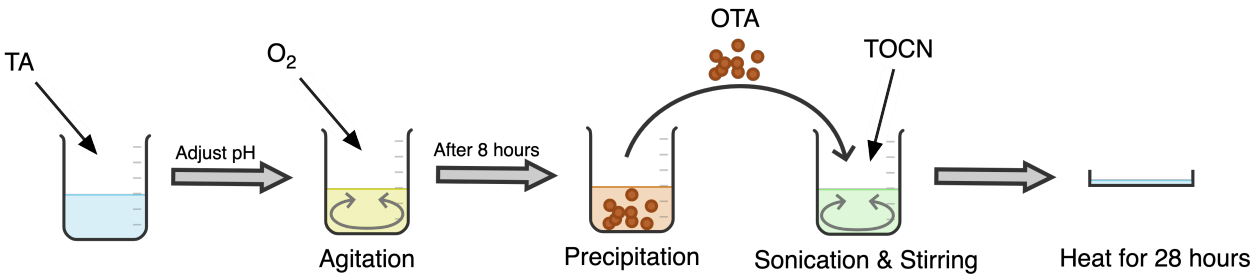

Figure 3.1: Overview of TOCN/OTA hydrogel synthesis from aqueous solution of tannic acid and TOCN suspension.

3.3.Characterization

3.3.1. SEM

The oxidized tannic acid particles and the TOCN/OTA hydrogels were imaged using a field-emission scanning electron microscope (Zeiss Gemini 500, Germany) operating at 1 kV. The OTA samples were prepared from an aqueous dispersion on silicon wafers. After blotting the suspension on a silicon chip, the coated sample was sputtered with a thin layer of palladium/gold alloy. The TOCN/OTA hydrogel samples were air-dried, freeze-dried (aerogel) and coated with a layer of palladium/gold alloy.

3.3.2. FTIR

FTIR spectra of OTA particles, a TOCN suspension, and TOCN/OTA aerogels were obtained with an ATR-FTIR Spectrometer (PerkinElmer). Each spectrum was collected between 600-4000 cm^{-1} at 4 cm^{-1} resolution using 32 scans.

3.3.3. TGA

TGA measurements of OTA particles, freeze-dried TOCN, and TOCN/OTA hydrogels were collected using the TA instrument TGA-Q500 under nitrogen flow (50 ml/min). The samples were scanned from room temperature up to 600 °C at a heating rate of 10 °C/min.

3.3.4. Rheological tests

The rheological tests of TOCN/OTA hydrogels were carried out with a rheometer (Advanced Rheometer, AR 2000) using a 60 mm parallel plate configuration at a gap distance of 1000 mm. The hydrogel sample was put on the bottom plate. After lowering the upper plate down under slow rotation upon touching the sample, the extra part of the hydrogel was removed, and the edge was cut vertically to the plate. The measurements were performed at room temperature (25 °C) and the whole test sequence took less than 40 minutes; thus, the evaporation of the sample was negligible.

Each measurement started with pre-shear at 1 s^{-1} for 10 s and subsequently rested for 5 min to reset the shear history of the sample. Frequency sweep and strain sweep were conducted to examine the gel-like behavior and probe the role of the dried TOCN/OTA weight ratio on the viscoelasticity of the resultant hydrogels. Frequency sweeps took place from 0.1 - 100 rad/s at a strain of 1% within the linear viscosity region. Strain amplitude sweeps were implemented using 0.1 - 100% at a frequency of 1 rad/s.

4. RESULTS AND DISCUSSION

4.1. Synthesis of Oxidized Tannic Acid Particles

Colloidal polyphenol particles were synthesized from aqueous solutions of tannic acid through a bottom-up method in alkaline conditions. The morphology control of the resultant particles is imperative to the manufacturing of functional composite materials. Kämäräinen et al. studied the effects of oxidation time, base species, and pH on the morphology of OTA particles including rods, platelets, rhomboids, cuboids, and quasi-spherical shapes. They proposed an inverse correlation between base counter cation ionic radius and particle volume, a direct correlations between initial pH and elongated morphologies, and a correlation between base strength and total yield.[54] In this work, we adjusted the pH to 7.8 by adding 1M NaOH aqueous solution. Kämäräinen et al. reported a difference in morphology between 14 hours and 1 week of oxidation time. We found noticeable precipitation after 8 hours of orbital shaking and a relatively consistent morphology between 8 – 14 hours. The variation in size of the oxidized particles and total precipitate yield increased with prolonged oxidation time. We adopted 8 hours of orbital shaking time for the oxidation step in order to have a more uniform morphology for the resulting OTA particles.

Unlike the light-yellow colored tannic acid powder, OTA particles had a dark green-brown color (Figure 4.1). Figure 4.2 shows the morphology of OTA particles obtained in the work. The dimension of the particles was approximately 16 μm in length and 8 μm in width. The particles had a structure of overlapped spindle-shaped oblate plates. Some of the particles assembled in different rotation and tilt angles hence forming flower-liked shapes.

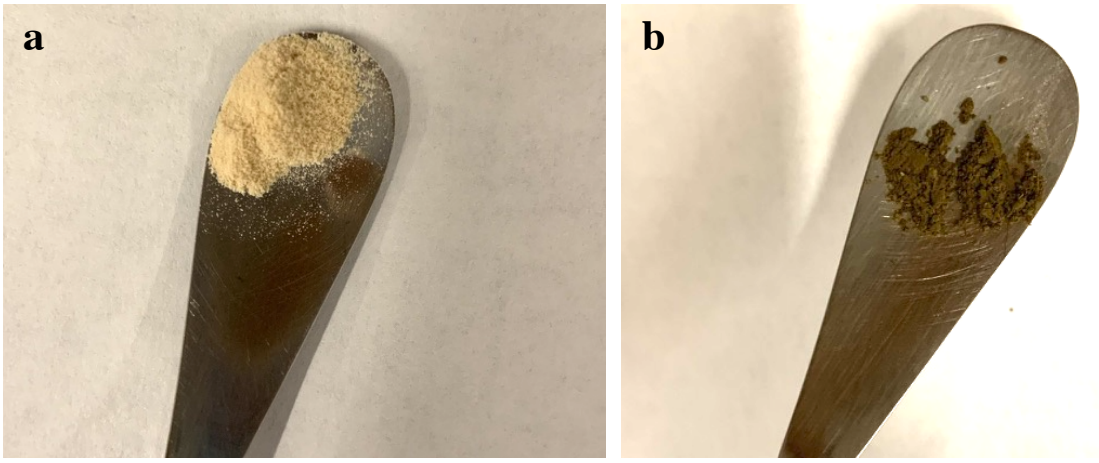

Figure 4.1: a) Tannic acid and b) oxidized tannic acid particles.

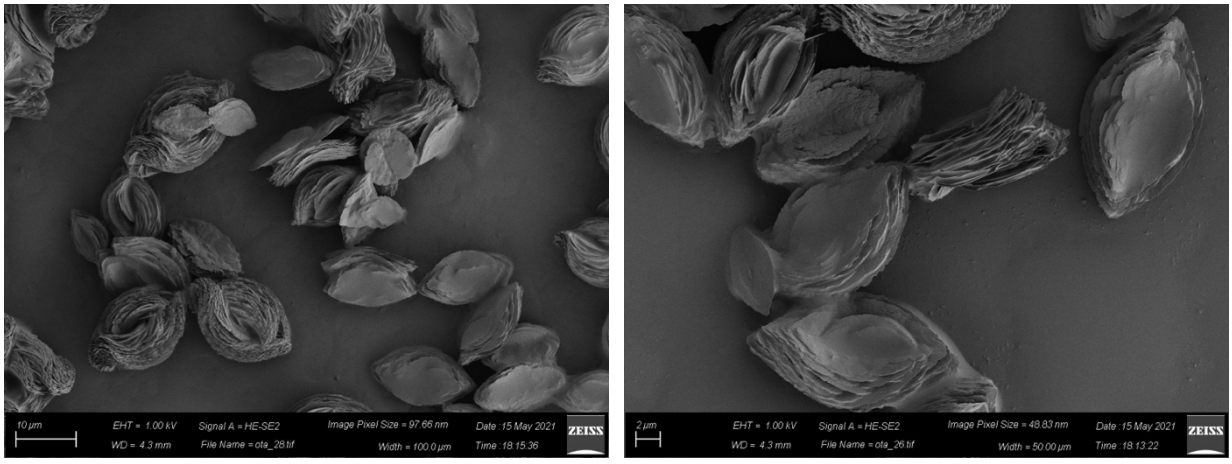

Figure 4.2: SEM images of oxidized tannic acid particles synthesized with 1M NaOH solution.

Fourier-transform infrared (FT-IR) spectroscopy indicates a change in the chemical makeup of oxidized tannic acid particles. In the OTA FTIR spectrum, the peak at 3250 cm^{-1} is attributed to O-H stretching, while the peak at 1698 is assigned to the C=O carbonyl stretching. The peaks at 1578, 1504 cm^{-1} correspond to the aromatic C=C-C vibrations. Peaks at 1458, 1396, 1340, 1288, 1196 cm^{-1} are assigned to C-O stretching, whereas peaks at 1100, 1040 cm^{-1} are assigned to aromatic in-plane C-H stretching. Our OTA FTIR spectrum agrees with that reported by Kämäräinen et al. which also included matrix-assisted laser desorption/ionization (MALDI) mass spectra of OTA particles revealing a galloyl residue.[54] The oxidation of tannic acid likely generates

ellagitannins and hexahydroxydiphenic acid units, and they found no evidence on the formation of ellagic acid.[55]

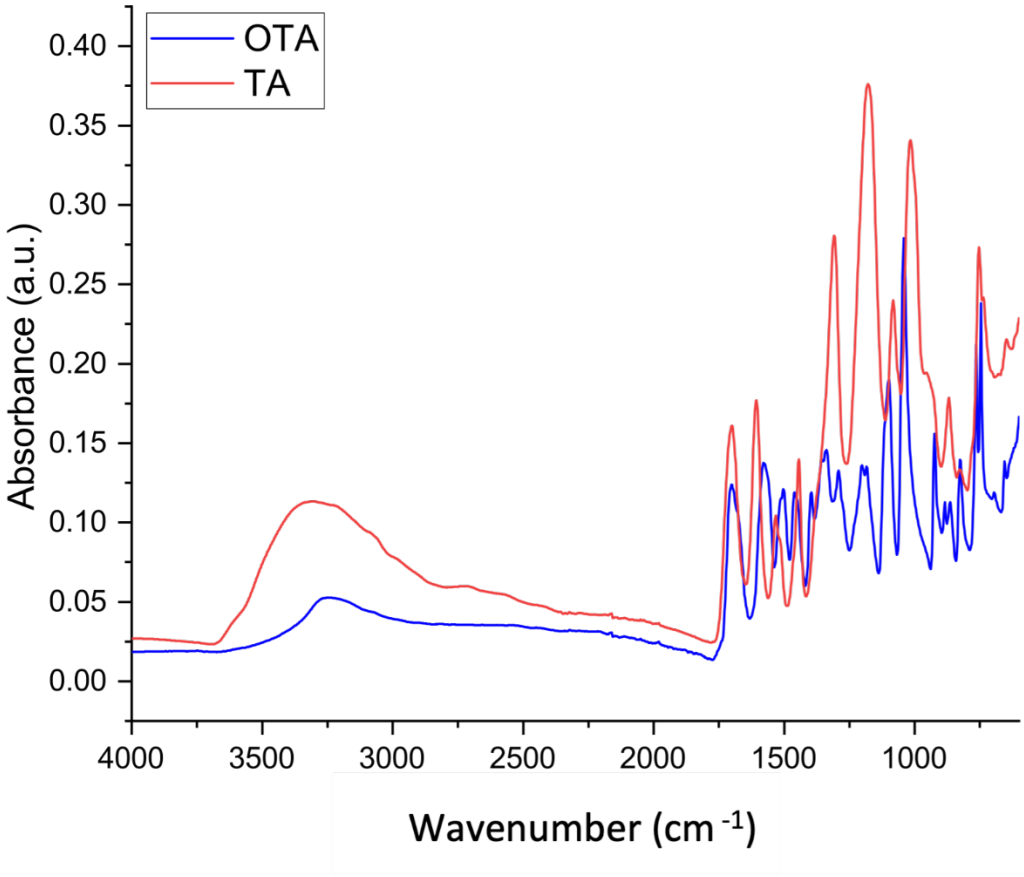

Figure 4.3: FTIR spectra of tannic acid and oxidized tannic acid particles.

We used Thermogravimetric Analysis (TGA) and Derivative Thermogravimetry (DTG) to investigate the thermal properties of tannic acid and oxidized tannic acid particle. We noticed that the onset of thermal degradation increased from ca. 230 to 430 °C after oxidation suggesting higher thermal stability in the galloyl-rich OTA particles.[55] The char content of the OTA specimen at 600 °C is almost half of its initial weight, which is about twice of that of the TA sample. This increase in thermal stability is likely attributed to a higher crystallinity in OTA particles.[54]

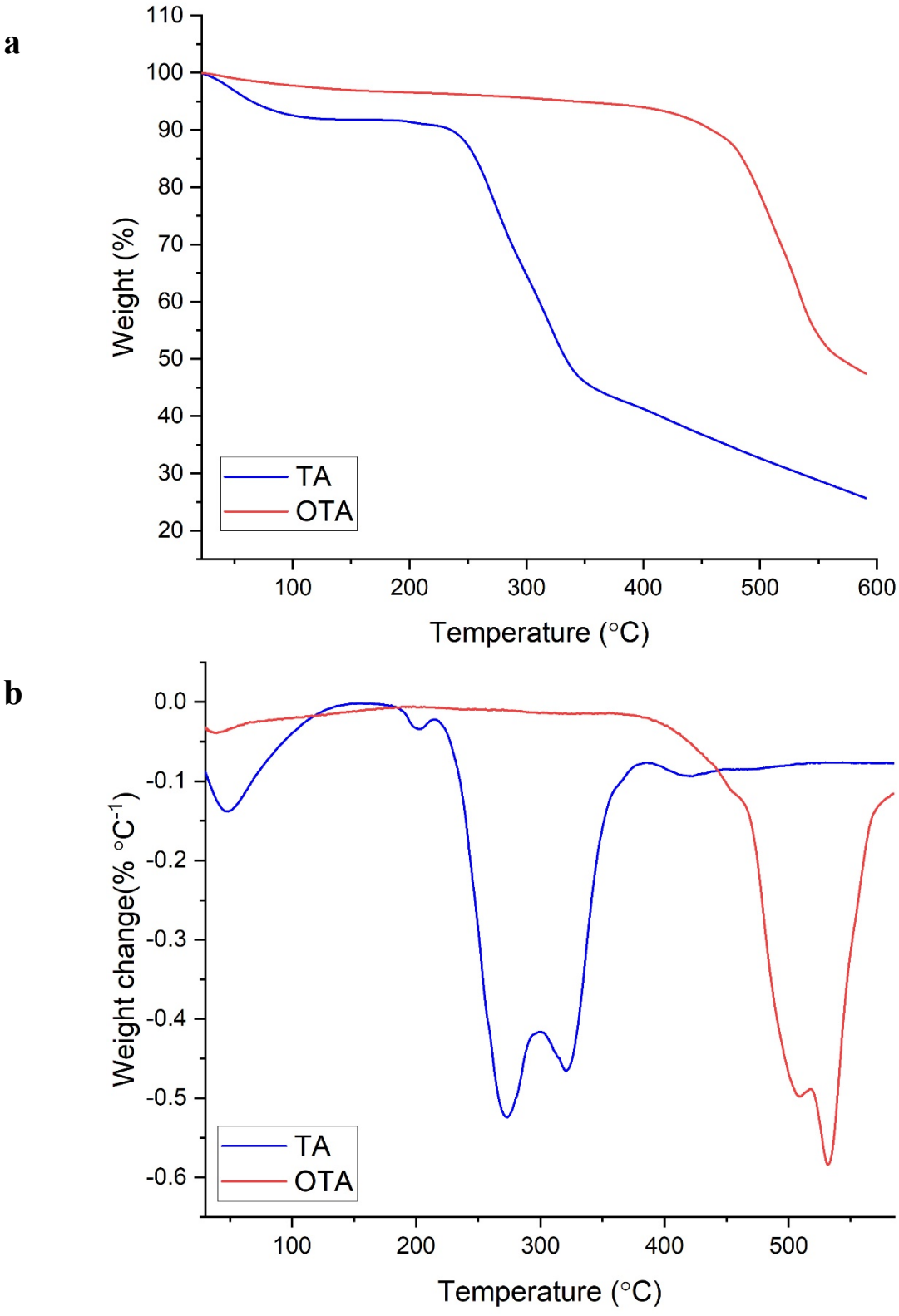

Figure 4.4: a) TGA and b) DTG for tannic acid and oxidized tannic acid particles.

4.2. Formation of TOCN/OTA Hydrogels

Since TOCN hydrogels contain a large amount of water, we also prepared TOCN aerogels for TGA measurements. TOCN is a relatively stable translucent suspension. (Figure 4.5a) After freeze-drying, we obtained a TOCN aerogel that was fluffy and of white color and took the shape of the vessel. Figure 4.5c shows a green-brown porous TOCN/OTA aerogel with a rough external surface.

Different from the TOCN suspension, the addition of OTA particles resulted in a solid non-fluidic gel. The green-brown color TOCN/OTA hydrogel was molded in a petri-dish. A higher concentration of OTA particles led to a darker color (Figure 4.5d).

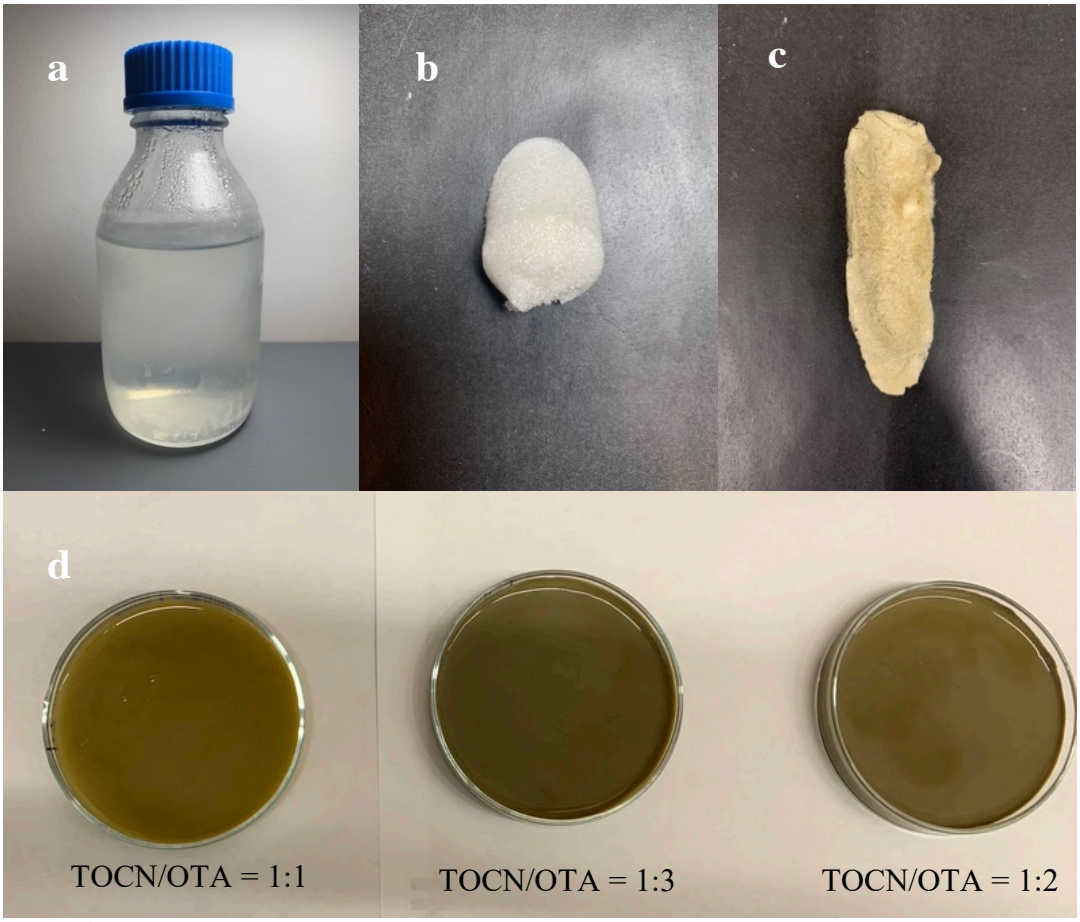

Figure 4.5: a) TOCN suspension. b) TOCN aerogel. c) TOCN/OTA aerogel prepared with a weight ratio of 1:2. d) TOCN/OTA hydrogels prepared with TOCN/OTA weight ratios of 1:1, 1:2, and 1:3.

Figure 4.6 shows the morphology of air-dried and freeze-dried TOCN/OTA aerogels prepared with a TOCN/OTA weight ratio of 1:3. The freeze-dried TOCN/OTA aerogel shows a sheet-like structure made of nanofibers with OTA particles inside and on the surface. The cellulose nanofibers are highly entangled with each other and tightly wound around OTA particles.

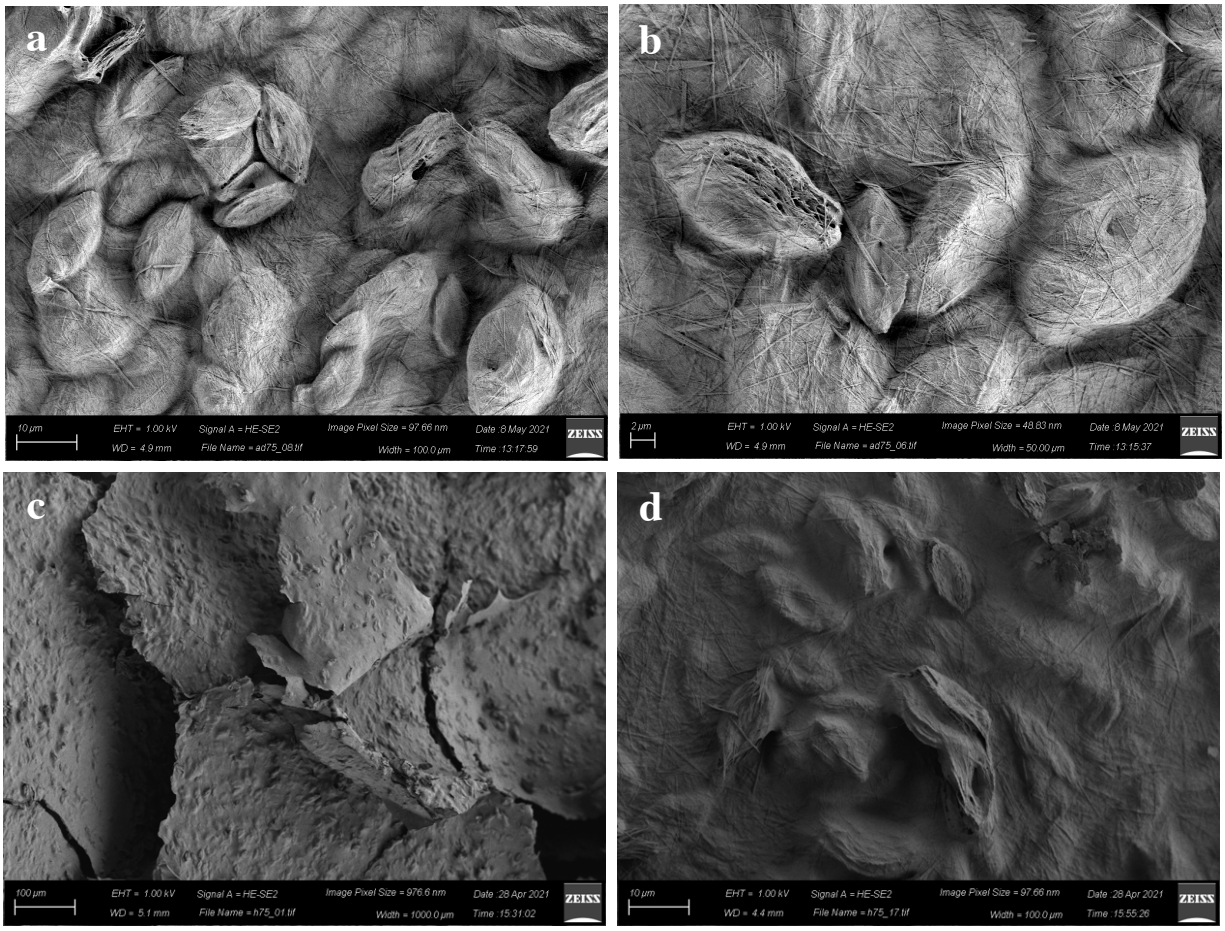

Figure 4.6: SEM images of a) and b) air-dried TOCN/OTA hydrogels, c) and d) freeze-dried TOCN/OTA aerogels.

Ovalle et al. discussed five main approaches for the preparation of hydrogels:

1. Forming hydrogels from nanoparticle suspensions.
2. Physically embedding nanoparticles into the hydrogel matrix after gelation.

3. Forming reactive nanoparticles within a gel.
4. Forming hydrogels by crosslinking nanoparticles.
5. Forming hydrogels with nanoparticles, polymers, and distinct gelating molecules.

The method we used for preparing TOCN/OTA hydrogels is similar to approach number 4, as we physically crosslinked TOCN and OTA particles by hydrogen bonds as shown in the FTIR spectra shown in Figure 4:7.

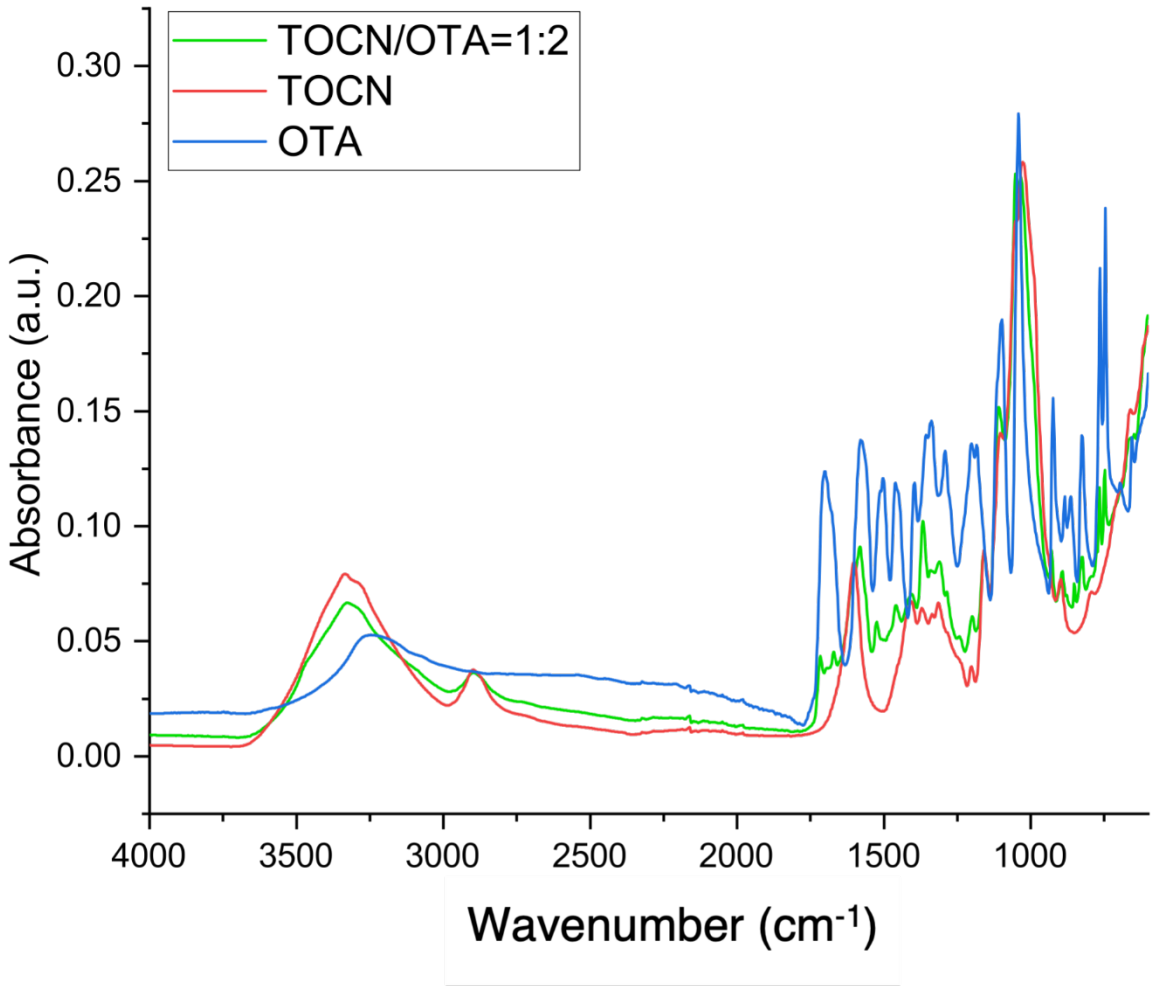

Figure 4.7: FTIR spectra for OTA particles, freeze-dried TOCN suspension, and TOCN/OTA aerogels.

Figure 4.7 shows the FTIR spectra of OTA, TOCN, and a TOCN/OTA hydrogel specimen prepared with a TOCN/OTA weight ratio of 1:2. The spectra of TOCN and the hydrogel show typical bands of cellulose. The main absorption peak at 3320 cm^{-1} can be attributed to O-H stretching. Peaks at 2900 cm^{-1} correspond to CH_2, while the typical peaks at 1600 and 1412 cm^{-1} correspond to the asymmetric and symmetric stretching mode for -OCO- groups.[56,57] The most intense band can be attributed to the C-O vibration of C2, C3, and C6 at 1046 cm^{-1}.[58] Additional peaks at 1716, 1672 cm^{-1} can be attributed to the C=O carbonyl stretching on OTA particles. Other peaks at 1526, 1462 cm^{-1}, and the increase of signals between 1428 and 1306 cm^{-1} can be attributed to C-O stretching on OTA. The spectrum of the hydrogel shows a typical band of cellulose and a superimposed combination of the TOCN and OTA signals.

TGA thermograms (Figure 4.8a) of the OTA, TOCN, and TOCN/OTA aerogel samples show an initial weight loss of ca. 4% for the TOCN/OTA aerogel, and a weight loss of ca. 7% for the TOCN aerogel. This initial mass loss may be due to humidity. The aerogels show two onsets of thermal degradation, suggesting the TOCN and OTA were physically crosslinked. The onsets correspond to the degradation of TOCN at ca. 185℃ and the degradation of OTA at ca. 400 ℃.

Figure 4.8b shows the DTG for OTA, TOCN, and TOCN/OTA aerogels. The DTF curve of TOCN aerogels exhibits a shoulder at 240 ℃ due to the decomposition of carboxylic units on the TOCN surface.[59,60] The shoulders in the curves of TOCN/OTA aerogels shift to ca. 250 ℃, and the decomposition temperature of TOCN shifts from 280 to 320 ℃. These shifts indicate improved thermal stability.

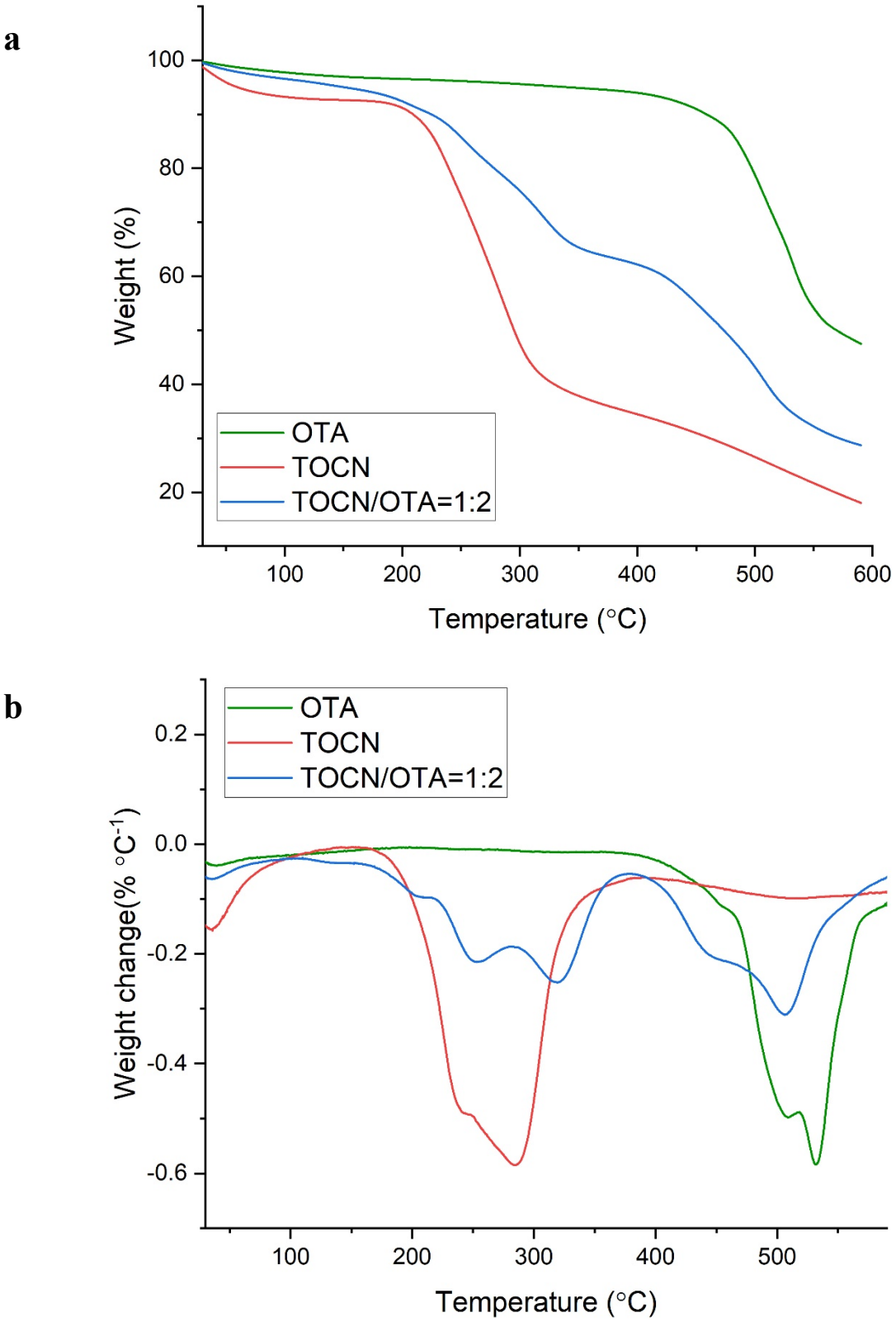

Figure 4.8: a) TGA and b) DTG for OTA particles, freeze-dried TOCN suspension, and TOCN/OTA aerogels.

4.3.Effect of TOCN/OTA Weight Ratios on Thermal and Mechanical Properties

Figure 4.9 shows the FTIR spectra of TOCN/OTA hydrogels prepared using three weight ratios (TOCN/OTA = 1:1, 1:2, 1:3). The spectra for hydrogels with ratios of 1:1 and 1:2 exhibit similar bands, while the hydrogel with a ratio of 1:3 shows a lower peak at of 3320 cm^{-1} and exhibits a shoulder at 3464 cm^{-1}. The peaks from 3700 to 3250 cm^{-1} indicate hydroxyl groups, which are considerably influenced by hydrogen bonding. As reported by Roberts et al., a sharp absorption band at 3700 cm^{-1} corresponds to a free or unassociated hydroxyl group, while a band at around 3350 cm^{-1} is characterized by hydrogen-bonded hydroxyl groups. A lower frequency relative to the position of the free hydroxyl group leads to a stronger hydrogen bond.[61] Therefore, we can conclude that the hydrogel with a TOCN/OTA ratio of 1:3 contains the least amount of hydrogen bonds. Furthermore, the TOCN/OTA=1:3 hydrogel shows the lowest peak in the range of 1160 to 1050 cm^{-1}, corresponding to C-O stretching on the carboxylate glucose units. It also shows an increased absorption intensity at 1714, and 1668 cm^{-1}, which can be attributed to C=O carbonyl stretching. Because of the higher amount of OTA particles added in the TOCN suspension for the hydrogel with a ratio of 1:3, the decrease of C-O vibration is likely resulted from the oxidation of hydroxyl groups on C6 to aldehyde groups.

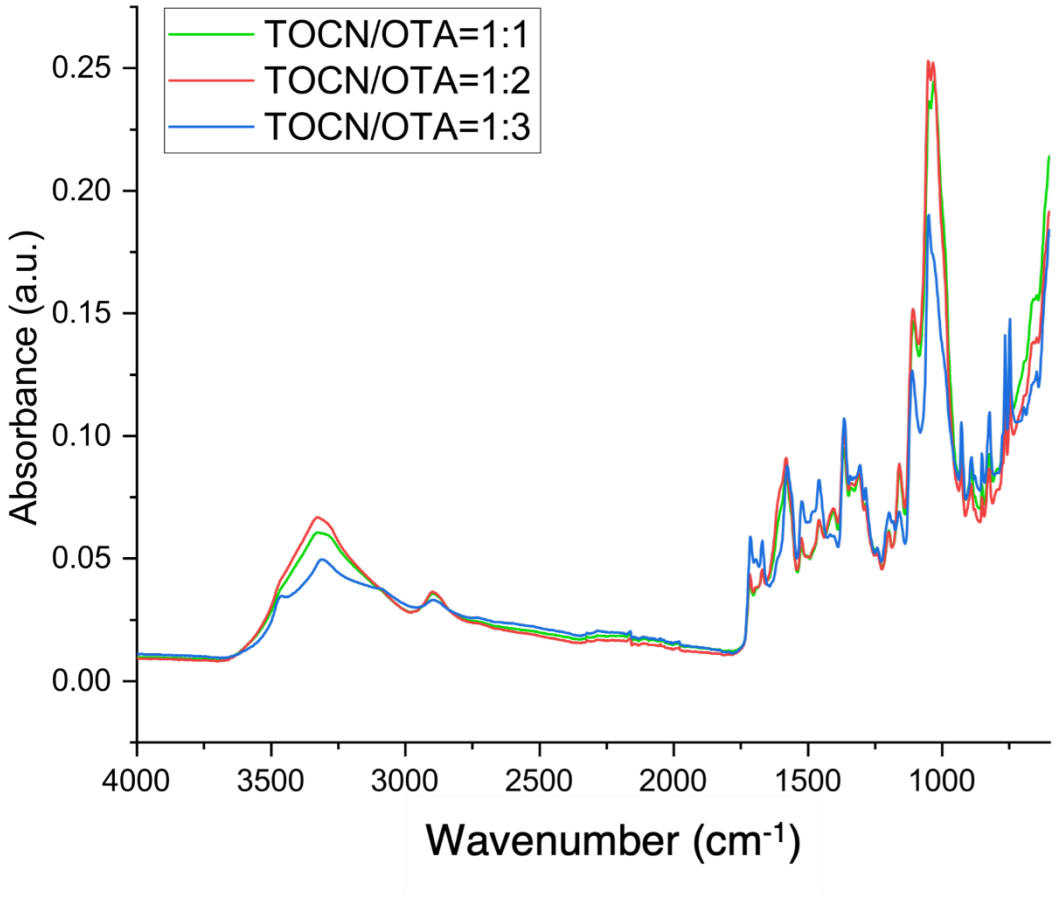

Figure 4.9: FTIR spectra for aerogels prepared with TOCN/OTA weight ratios of 1:1, 1:2, and 1:3.

Figure 4.10 shows the TGA and DTG spectra for TOCN/OTA aerogels with 1:1, 1:2, and 1:3 weight ratios. The thermogram of the aerogel with a TOCN/OTA ratio of 1:1 shows the highest weight loss of around 38%, while those of the other two aerogels present a weight loss of 25% due to the degradation of TOCN. The resultant aerogels started the second period of degradation at ca. 400 °C, which is attributed to the OTA particles incorporated. All three samples had weight loss higher than 27%. The thermograms for hydrogels with a TOCN/OTA ratio of 1:2 and 1:3, after reaching 600 °C, show higher char contents than the hydrogel with a lower.[54]

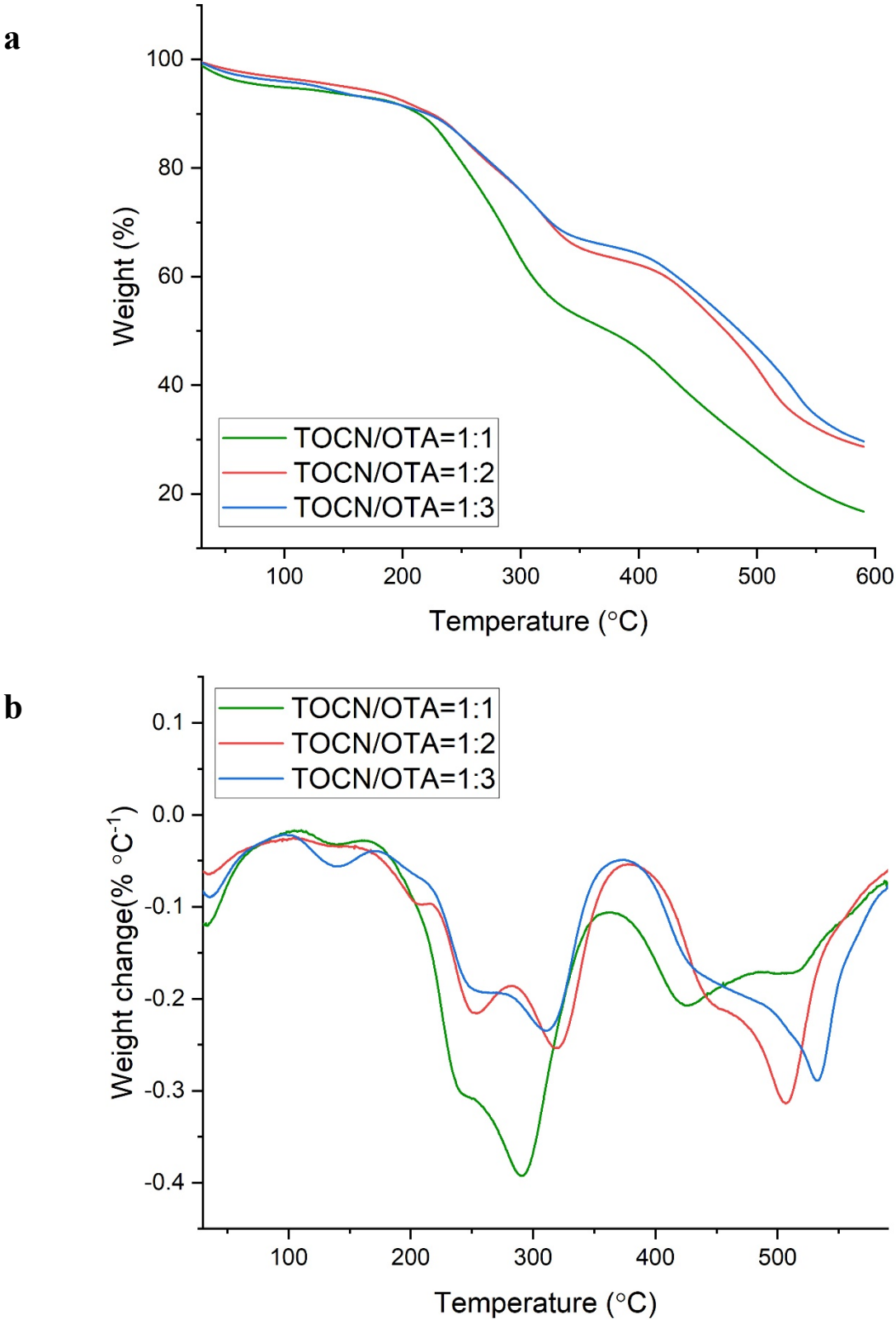

Figure 4.10: a) TGA and b) DTG for aerogels prepared with TOCN/OTA weight ratios of 1:1, 1:2, and 1:3.

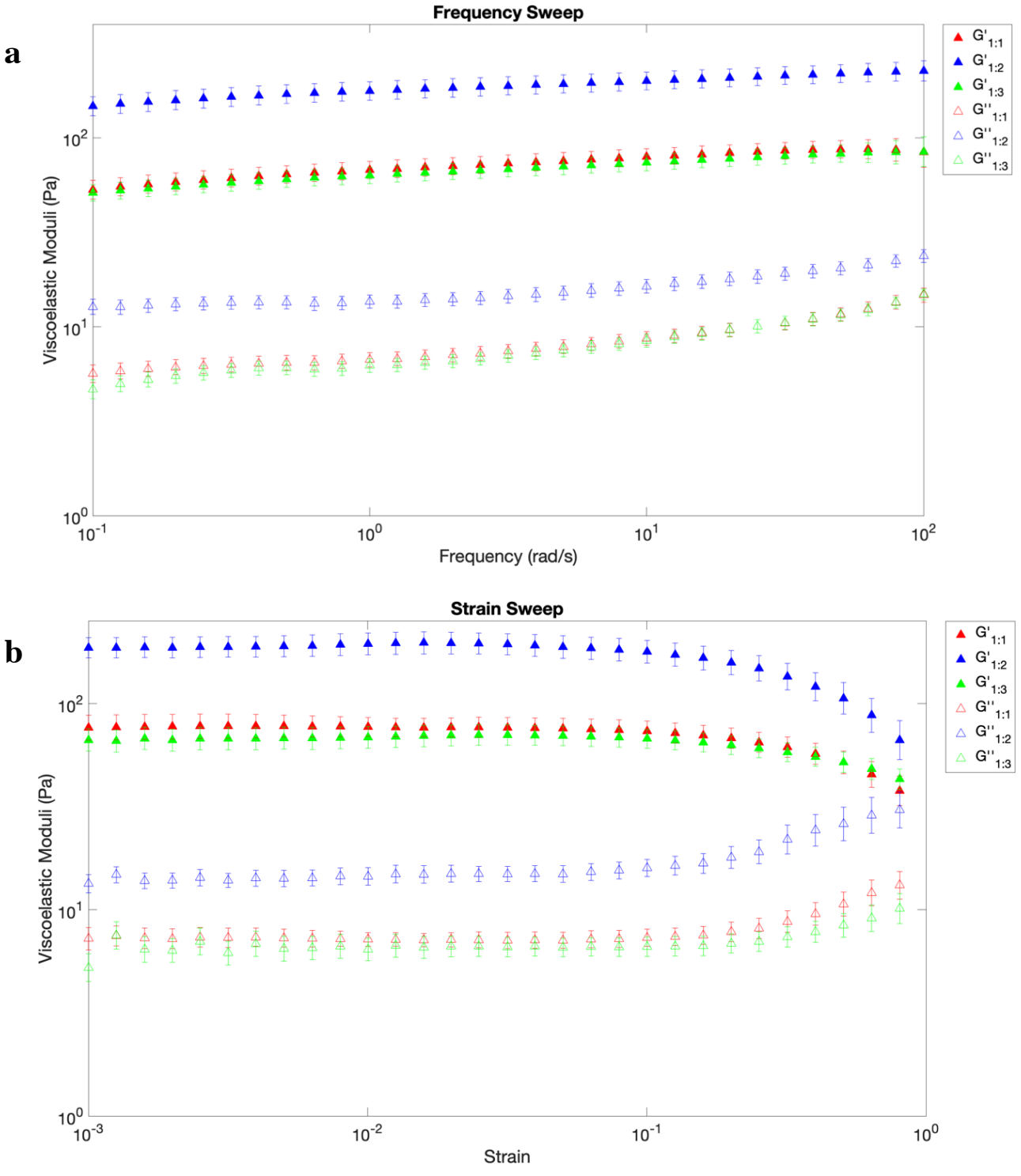

Figure 4.11: a) frequency sweep and b) strain sweep measurements at 25 °C for hydrogels prepared with TOCN/OTA weight ratios of 1:1, 1:2, and 1:3.

The mechanical properties of hydrogels are critical parameters for manufacturing, storage, and application of these materials. These properties are tunable by using crosslinking agents, changing formulations, and altering gelation conditions. Rheological measurements are quick and sensitive approaches to characterize hydrogels' mechanical properties, architecture, crosslinking degree, structural homogeneity/heterogeneity, and molecular weight.[62] Since the TOCN/OTA hydrogels are fragile, we used the small-amplitude oscillatory shear (SAOS) technique and kept the strains relatively low to avoid destroying or modifying the samples.

The rheological behavior of the TOCN/OTA hydrogels is shown in Fig 4.11a. Frequency sweep measurements were performed under 1% strain, within the linear-viscoelastic (LVE) regime. Fig 4.11a shows that between 0.1 and 100 rad/s, the storage modulus (G') for all three samples was an order of magnitude higher than the loss modulus (G''), indicating that the specimens mostly behaved like elastic solids under cyclical deformation. The moduli (G' and G'') of these materials show little frequency dependency, indicating enhanced mechanical stability of the hydrogels. A plateau was not observed at low frequency, suggesting that an equilibrium modulus was not presented.[63] The elastic behavior of the resultant hydrogels is attributed to weak crosslink interactions such as hydrogen bonds and van der Waals forces.[64]

In particular, the hydrogel sample prepared with the weight ratio of 1:2 presented higher values for storage modulus in contrast to the other two samples with ratios of 1:1 and 1:3. We speculate that an optimal TOCN/OTA weight ratio for a maximum storage modulus exists around 1:2.[65] The variability in the storage and loss moduli of hydrogels could be assigned to aggregation of OTA particles and an increased crosslinking density when the concentration of OTA is high.[66]

Strain sweep measurements further probe the viscoelastic behavior of the gel under increasing cyclical deformations. The strain sweep profiles in Figure 4.11b show that the hydrogel prepared with a TOCN/OTA weight ratio of 1:2 exhibited the highest values of storage and loss moduli. Moreover, the curves confirmed that all of three hydrogels remained in their linear viscoelastic regime under the strain of 0.1. After that value of strain, their storage moduli started to decay, and the loss modulus increased. This indicates that the network structure of the prepared hydrogels is relatively weak and easily breakable comparing to other cellulose-based hydrogels. [30,31]

5. CONCLUSIONS

Using only water as the solvent, we successfully prepared hydro and aerogels from TOCN and OTA particles using a 'one-pot' method. We controlled the morphologies and dimensions of OTA particles in the precipitation process. The oxidation of TA resulted in galloyl-rich OTA particles with an elevated thermal stability. OTA particles were physically crosslinked with TOCN via inter- and intramolecular hydrogen bonds. Microscopy measurements showed that cellulose nanofibers compactly wound around the OTA particles and constructed a highly entangled structure.

Furthermore, we discussed the role of the TOCN/OTA weight ratio on hydrogel formation and the mechanical and thermal properties of the hydrogels. The rheological analysis investigated the viscoelastic behavior of hydrogels with different TOCN/OTA weight ratios. TOCN/OTA hydrogels behaved like elastic solids and were relatively stable under cyclic deformation. The hydrogel prepared at a TOCN/OTA weight ratio of 1:2 exhibited the highest values of storage and loss moduli. TGA thermograms showed that samples with ratios of 1:2 and 1:3 shared similar and improved thermal properties. We speculate that an optimal TOCN/OTA weight ratio for the enhanced mechanical and thermal properties exists, as the hydrogel prepared at a ratio of 1:2 was stronger and more stable than hydrogels with 1:1 and 1:3 weight ratios.[65]

6. RECOMMENDATIONS FOR FUTURE WORK

For this work, we chose to use spindle-liked OTA particles synthesized with NaOH at pH 7.8 after 8 hours of orbital shaking. Future researcher might experiment with other morphologies of OTA, such as cuboidal, odd-shaped, needle, rod-liked, and dumbbell-liked particles which are obtained under different oxidation conditions.[54] Moreover, we adopted a shorter time for oxidation to obtain more consistent morphologies and dimensions of OTA; the effect of the size distribution of the particles can be investigated and narrowed in a future work. Since the OTA particles used in this work have a low surface area compared to that of cellulose nanofibers, increasing the surface area and tuning the size of the OTA particles can further improve their mechanical properties. We prepared three different weight ratios of TOCN/OTA to probe the effect of the concentration of OTA particles on the mechanical and thermal properties of hydrogels. We deduced that an optimal weight ratio should exist around a 1:2 TOCN/OTA ratio, though additional work is needed to determine the precise value or a narrower range. The reason for the reduced presence of hydrogen bonds, and hence, a decrease in mechanical properties of hydrogels prepared at the 1:3 TOCN/OTA ratio, is likely due to the change of chemical structure on the surface of cellulose as the FTIR measurements show. The reactions occurred when that happened remain unclear, therefore, other analyses such as MALDI can be applied to probe those mechanisms.

Various biological and chemical analyses could be applied to explore possible functions of hydrogels. Although these TOCN/OTA hydrogels are free-standing, they are still considered to be weak and brittle compared to other cellulose-based composite hydrogels. [30,31] The weak network is largely attributed to the physical crosslinks present in the structure; therefore, introducing stronger inter- and intramolecular interactions through the addition of additives or crosslinking agents holds promise for improving their properties. Moreover, only one variable was probed in this work: TOCN/OTA ratio. Other important parameters such as heating temperature, time, and pH could be investigated to tailor the properties and tune them to address other functions of these hydrogels.

7. REFERENCES

1. Ahmed, E. M. Hydrogel: Preparation, characterization, and applications: A review. *Journal of Advanced Research* vol. 6 105–121 (2015).
2. Ajdary, R., Tardy, B. L., Mattos, B. D., Bai, L. & Rojas, O. J. Plant Nanomaterials and Inspiration from Nature: Water Interactions and Hierarchically Structured Hydrogels. *Adv. Mater.* **2001085**, (2020).
3. Koopmann, A. K. *et al.* Tannin-Based Hybrid Materials and Their Applications: A Review. *Molecules (Basel, Switzerland)* vol. 25 4910 (2020).
4. Qi, H. *Novel Functional Materials Based on Cellulose.* (Springer International Publishing, 2017). doi:10.1007/978-3-319-49592-7.
5. Zugenmaier, P. History of Cellulose Research. in *Crystalline Cellulose and Cellulose Derivatives: Characterization and Structure* 7–51 (Springer-Verlag Berlin Heidelberg, 2008). doi:10.1007/978-3-540-73934-0.
6. Klemm, D. *et al.* Nanocelluloses: A new family of nature-based materials. *Angewandte Chemie - International Edition* vol. 50 5438–5466 (2011).
7. Pizzi, A. Tannins: Major Sources, Properties and Applications. Monomers, *Polym. Compos. from Renew. Resour.* 179–199 (2008) doi:10.1016/B978-0-08-045316-3.00008-9.
8. Dufresne, A. Nanocellulose: A new ageless bionanomaterial. *Materials Today* vol. 16 220–227 (2013).
9. Moon, R. J., Martini, A., Nairn, J., Simonsen, J. & Youngblood, J. Cellulose nanomaterials review: structure, properties and nanocomposites. *Chem. Soc. Rev* 40, 3941–3994 (2011).
10. Lavoine, N., Desloges, I., Dufresne, A. & Bras, J. Microfibrillated cellulose - Its barrier properties and applications in cellulosic materials: A review. *Carbohydrate Polymers* vol. 90 735–764 (2012).
11. Klemm, D. *et al.* Nanocellulose as a natural source for groundbreaking applications in materials science: Today's state. *Materials Today* vol. 21 720–748 (2018).
12. Yang, X. *et al.* Surface and Interface Engineering for Nanocellulosic Advanced Materials. *Adv. Mater.* 2002264 (2020) doi:10.1002/adma.202002264.
13. Dufresne, A. *Nanocellulose : From Nature to High Performance Tailored Materials.* (ProQuest Ebook Central, 2017).
14. Dufresne, A. 5 Chemical modification of nanocellulose. in Nanocellulose (DE

GRUYTER, 2012). doi:10.1515/9783110254600.147.

15. Habibi, Y., Chanzy, H. & Vignon, M. R. TEMPO-mediated surface oxidation of cellulose whiskers. *Cellulose* 13, 679–687 (2006).

16. Okita, Y., Fujisawa, S., Saito, T. & Isogai, A. TEMPO-Oxidized Cellulose Nanofibrils Dispersed in Organic Solvents. doi:10.1021/bm101255x.

17. Bragd, P. L., Besemer, A. C. & Van Bekkum, H. Bromide-free TEMPO-mediated oxidation of primary alcohol groups in starch and methyl α-D-glucopyranoside. *Carbohydr. Res.* 328, 355–363 (2000).

18. Okita, Y., Fujisawa, S., Saito, T. & Isogai, A. TEMPO-oxidized cellulose nanofibrils dispersed in organic solvents. *Biomacromolecules* 12, 518–522 (2011).

19. Geng, L. *et al.* Structure characterization of cellulose nanofiber hydrogel as functions of concentration and ionic strength. *Cellulose* 24, 5417–5429 (2017).

20. Liao, J., Pham, K. A. & Breedveld, V. Rheological characterization and modeling of cellulose nanocrystal and TEMPO-oxidized cellulose nanofibril suspensions. *Cellulose* 27, 3741–3757 (2020).

21. Masruchin, N., Park, B. D., Causin, V. & Um, I. C. Characteristics of TEMPO-oxidized cellulose fibril-based hydrogels induced by cationic ions and their properties. *Cellulose* 22, 1993–2010 (2015).

22. Sone, A., Saito, T. & Isogai, A. Preparation of Aqueous Dispersions of TEMPO-Oxidized Cellulose Nanofibrils with Various Metal Counterions and Their Super Deodorant Performances. *ACS Macro Lett.* 5, 1402–1405 (2016).

23. Al-Ahmed, Z. A., Hassan, A. A., El-Khouly, S. M. & El-Shafey, S. E. TEMPO-oxidized cellulose nanofibers/TiO2 nanocomposite as new adsorbent for Brilliant Blue dye removal. *Polym. Bull.* 77, 6213–6226 (2020).

24. Kurihara, T. & Isogai, A. Properties of poly(acrylamide)/TEMPO-oxidized cellulose nanofibril composite films. *Cellulose* 21, 291–299 (2014).

25. Masruchin, N., Park, B. D. & Causin, V. Dual-responsive composite hydrogels based on TEMPO-oxidized cellulose nanofibril and poly(N-isopropylacrylamide) for model drug release. *Cellulose* 25, 485–502 (2018).

26. Yamada, T. *et al.* Growth of dispersed hydroxyapatite crystals highly intertwined with TEMPO-oxidized cellulose nanofiber. *CrystEngComm* 22, 4933–4941 (2020).

27. Siqueira, P. *et al.* Three-Dimensional Stable Alginate-Nanocellulose Gels for Biomedical Applications: Towards Tunable Mechanical Properties and Cell Growing. *Nanomaterials*

9, 78 (2019).

28. Abouzeid, R. E., Khiari, R., Beneventi, D. & Dufresne, A. Biomimetic Mineralization of Three-Dimensional Printed Alginate/TEMPO-Oxidized Cellulose Nanofibril Scaffolds for Bone Tissue Engineering. *Biomacromolecules* 19, 4442–4452 (2018).

29. Niu, J., Wang, J., Dai, X., Shao, Z. & Huang, X. Dual physically crosslinked healable polyacrylamide/cellulose nanofibers nanocomposite hydrogels with excellent mechanical properties. *Carbohydr. Polym.* 193, 73–81 (2018).

30. Lu, Y. *et al.* TEMPO-oxidized cellulose nanofibers/polyacrylamide hybrid hydrogel with intrinsic self-recovery and shape memory properties. *Cellulose* 1–20 (2021) doi:10.1007/s10570-020-03606-8.

31. Mihranyan, A. Viscoelastic properties of cross-linked polyvinyl alcohol and surface-oxidized cellulose whisker hydrogels. *Cellulose* 20, 1369–1376 (2013).

32. Shefa, A. A. *et al.* Curcumin incorporation into an oxidized cellulose nanofiber-polyvinyl alcohol hydrogel system promotes wound healing. *Mater. Des.* 186, 108313 (2020).

33. Mueller-Harvey, I. Analysis of hydrolysable tannins. *Anim. Feed Sci. Technol.* 91, 3–20 (2001).

34. Schofield, P., Mbugua, D. M. & Pell, A. N. Analysis of condensed tannins: A review. *Animal Feed Science and Technology* vol. 91 21–40 (2001).

35. Shirmohammadli, Y., Efhamisisi, D. & Pizzi, A. Tannins as a sustainable raw material for green chemistry: A review. *Industrial Crops and Products* vol. 126 316–332 (2018).

36. Hemingway, Richard W., J. J. . K. *Chemistry and Significance of Condensed Tannins.* (Springer, Boston, MA, 1989). doi:10.1007/978-1-4684-7511-1.

37. Kämäräinen, T. *et al.* Morphology-Controlled Synthesis of Colloidal Polyphenol Particles from Aqueous Solutions of Tannic Acid. *ACS Sustain. Chem. Eng.* 7, 16985–16990 (2019).

38. Yang, J. *et al.* Double Cross-Linked Chitosan Composite Films Developed with Oxidized Tannic Acid and Ferric Ions Exhibit High Strength and Excellent Water Resistance. (2019) doi:10.1021/acs.biomac.8b01420.

39. Ge, S. *et al*. Coordination of Covalent Cross-Linked Gelatin Hydrogels via Oxidized Tannic Acid and Ferric Ions with Strong Mechanical Properties. (2019) doi:10.1021/acs.jafc.9b03947.

40. Gülçin, I., Huyut, Z., Elmastaş, M. & Aboul-Enein, H. Y. Radical scavenging and antioxidant activity of tannic acid. *Arab. J. Chem.* 3, 43–53 (2010).

41. Aswathy Aromal, S. & Philip, D. Facile one-pot synthesis of gold nanoparticles using tannic acid and its application in catalysis. *Phys. E Low-Dimensional Syst. Nanostructures* 44, 1692–1696 (2012).

42. Bance, R. E. & Teel, R. W. Effect of tannic acid on rat liver S9 mediated mutagenesis, metabolism and DNA binding of benzo[a]pyrene. *Cancer Lett.* 47, 37–44 (1989).

43. Khan, W. A., Wang, Z. Y., Athar, M., Bickers, D. R. & Mukhtar, H. Inhibition of the skin tumorigenicity of (±)-7β,8α-dihydroxy-9α,10α-epoxy-7,8,9,10-tetrahydrobenzo[a]pyrene by tannic acid, green tea polyphenols and quercetin in Sencar mice. *Cancer Lett.* 42, 7–12 (1988).

44. Liu, L. *et al*. Tannic acid-modified silver nanoparticles for enhancing anti-biofilm activities and modulating biofilm formation. *Biomater. Sci.* 8, 4852–4860 (2020).

45. Fan, H. *et al.* Supramolecular Hydrogel Formation Based on Tannic Acid. (2017) doi:10.1021/acs.macromol.6b02106.

46. Hao, S. *et al.* Tannic Acid−Silver Dual Catalysis Induced Rapid Polymerization of Conductive Hydrogel Sensors with Excellent Stretchability, Self-Adhesion, and Strain-Sensitivity Properties. *Cite This ACS Appl. Mater. Interfaces* 12, 56521 (2020).

47. Chen, Y.-N. *et al.* Poly(vinyl alcohol)−Tannic Acid Hydrogels with Excellent Mechanical Properties and Shape Memory Behaviors. *ACS Appl. Mater. Interfaces* 8, 2021 (2016).

48. Hong, K. H. Polyvinyl alcohol/tannic acid hydrogel prepared by a freeze-thawing process for wound dressing applications. *Polym. Bull.* 74, 2861–2872 (2017).

49. Hong, K. H. Preparation and properties of polyvinyl alcohol/tannic acid composite film for topical treatment application. *Fibers Polym.* 17, 1963–1968 (2016).

50. Hu, Z., Berry, R. M., Pelton, R. & Cranston, E. D. One-Pot Water-Based Hydrophobic Surface Modification of Cellulose Nanocrystals Using Plant Polyphenols. (2017) doi:10.1021/acssuschemeng.7b00415.

51. Shao, C. *et al.* Mussel-Inspired Cellulose Nanocomposite Tough Hydrogels with Synergistic Self-Healing, Adhesive, and Strain-Sensitive Properties. *Chem. Mater.* 30, 3110–3121 (2018).

52. Shao, C. *et al.* Mimicking Dynamic Adhesiveness and Strain-Stiffening Behavior of Biological Tissues in Tough and Self-Healable Cellulose Nanocomposite Hydrogels. *ACS Appl. Mater. Interfaces* 11, 17 (2019).

53. Shrestha, S. *et al.* Surface hydrophobization of TEMPO-oxidized cellulose nanofibrils (CNFs) using a facile, aqueous modification process and its effect on properties of epoxy nanocomposites. *Cellulose* 26, 9631–9643 (2019).

54. Kämäräinen, T. *et al.* Morphology-Controlled Synthesis of Colloidal Polyphenol Particles from Aqueous Solutions of Tannic Acid. ACS Sustain. *Chem. Eng.* 7, 16985–16990 (2019).

55. Kaur Bhangu, S., Singla, R., Colombo, E., Ashokkumar, M. & Cavalieri, F. Green Chemistry COMMUNICATION Sono-transformation of tannic acid into biofunctional ellagic acid micro/nanocrystals with distinct morphologies †. *Green Chem.* 20, (2018).

56. Kafy, A. *et al.* Cellulose long fibers fabricated from cellulose nanofibers and its strong and tough characteristics. *Sci. Rep.* 7, 1–8 (2017).

57. Muthulakshmi, L. *et al.* Experimental Investigation of Cellulose/Silver Nanocomposites Using In Situ Generation Method. J. *Polym. Environ.* 25, 1021–1032 (2017).

58. Postek, M. T. *et al.* Development of the metrology and imaging of cellulose nanocrystals. *Meas. Sci. Technol. Meas. Sci. Technol* 22, 24005–24015 (2011).

59. Jiang, F. & Hsieh, Y. Lo. Self-assembling of TEMPO Oxidized Cellulose Nanofibrils As Affected by Protonation of Surface Carboxyls and Drying Methods. *ACS Sustain. Chem. Eng.* 4, 1041–1049 (2016).

60. Ovalle-Serrano, S. A., Gómez, F. N., Blanco-Tirado, C. & Combariza, M. Y. Isolation and characterization of cellulose nanofibrils from Colombian Fique decortication by-products. *Carbohydr. Polym.* 189, 169–177 (2018).

61. *Roberts, J. D.; Caserio, M. C. Spectroscopic Properties of Alcohols https://chem.libretexts.org/@go/page/22264 (2021).*

62. Zuidema, J. M., Rivet, C. J., Gilbert, R. J. & Morrison, F. A. A protocol for rheological characterization of hydrogels for tissue engineering strategies. J. Biomed. Mater. *Res. - Part B Appl. Biomater.* 102, 1063–1073 (2014).

63. Dong, H., Snyder, J. F., Williams, K. S. & Andzelm, J. W. Cation-induced hydrogels of cellulose nanofibrils with tunable moduli. *Biomacromolecules* 14, 3338–3345 (2013).

64. Chen, Y.-N., Jiao, C., Zhao, Y., Zhang, J. & Wang, H. Self-Assembled Polyvinyl Alcohol−Tannic Acid Hydrogels with Diverse Microstructures and Good Mechanical Properties. (2018) doi:10.1021/acsomega.8b02041.

65. Ma, T. *et al.* Rheological behavior and particle alignment of cellulose nanocrystal and its composite hydrogels during 3D printing. Carbohydr. *Polym.* 253, 117217 (2021).

66. Thoniyot, P., Tan, M. J., Karim, A. A., Young, D. J. & Loh, X. J. Nanoparticle–Hydrogel Composites: Concept, Design, and Applications of These Promising, Multi-Functional *Materials. Advanced Science* vol. 2 1400010 (2015)